Electron spin-resonance (ESR) and electron-nuclear double-resonance (ENDOR) study of the self-trapped hole in $ZnWO_4$ single crystals

2001 J. Phys.: Condens. Matter 13 1595

(http://iopscience.iop.org/0953-8984/13/7/320)

INSTITUTE OF PHYSICS PUBLISHING JOURNAL OF PHYSICS: CONDENSED MATTER

J. Phys.: Condens. Matter **13** (2001) 1595–1607 www.iop.org/Journals/cm PII: S0953-8984(01)18514-0

Electron spin-resonance (ESR) and electron–nuclear double-resonance (ENDOR) study of the self-trapped hole in $ZnWO_4$ single crystals

A Watterich[1], L Kovács[1], R Würz[2], F Schön[2], A Hofstaetter[2] and A Scharmann[2]

[1] Crystal Physics Laboratory, Research Institute for Solid State Physics and Optics, Hungarian Academy of Sciences, Konkoly-Thege M út 29-33, 1121 Budapest, Hungary
[2] 1. Physics Institute, Justus-Liebig-University, Heinrich-Buff-Ring 16, 35392 Giessen, Germany

E-mail: watter@power.szfki.kfki.hu (A Watterich)

Received 31 October 2000, in final form 11 January 2001

Abstract

After x-ray irradiation at 20 K, an intrinsic O^- centre was identified by ESR and ENDOR spectroscopy as the self-trapped hole centre in $ZnWO_4$. Observation of one Zn and two strong W superhyperfine interactions allows us to distinguish between two possible trapping sites: the hole resides at the B-type oxygen position which has one Zn and two W nearest neighbours. Broadening of the ESR lines and averaging of the g-value is observed and explained as due to thermally activated hopping of the hole between two energetically equivalent oxygen positions. The activation energy of this reorientation is found to be 0.016 ± 0.003 eV. The thermal decay of the intrinsic O^- centre, and its connection to thermoluminescence, has been studied; it shows that this centre cannot be the luminescence centre for the typical TL emission at $\sim$480 nm in $ZnWO_4$. This emission may be due to an intrinsic electron-type defect.

1. Introduction

Scintillator crystals are widely used as x-ray, γ-ray and particle detectors. The technological interest in the scintillator $ZnWO_4$ is due to its high conversion efficiency, supported also by high density, making this material a strong absorber of different radiations [1,2]. Under UV or x-ray irradiation, $ZnWO_4$ crystals emit light at about 480 nm (measured at 300 K) [3, 4]. This characteristic blue-green luminescence has been studied in detail and shown to be intrinsic [3, 4]. Molybdenum, being in the same column of the periodic table as W and thus a persistent impurity residing on ordinary tungsten sites, was proven to be the origin of an additional strong and broad emission band peaking at about 635 nm, having a long decay time and therefore being detrimental in some applications [5].

Since the thermoluminescence (TL) emission of $ZnWO_4$ is in the same blue-green region as the luminescence after UV or x-ray excitation, it is very likely that similar processes take

place in the two mechanisms. The photoluminescence and TL of $ZnWO_4$ have been extensively studied; however, the structure of the point defects involved is still not known [4,6]. Therefore the identification of the centres is essential to the understanding of the TL processes.

Various studies on point defects have clarified the nature of the impurity ions and the radiation-induced centres in $ZnWO_4$. The ESR results on divalent and trivalent metal dopants like Mn^{2+}, Co^{2+}, Ni^{2+}, Cu^{2+}, Fe^{3+} and Cr^{3+} substituting for Zn^{2+} with C_2 symmetry are summarized in reference [4]. All of these transition metal ions (except Ni) were shown to be present in undoped $ZnWO_4$ in low concentrations. Also, one finds Pt^{3+} and Rh^{2+}, obviously coming from the crucible [7]. Fe^{2+} and Cr^{3+} ions have optical absorption in the range of the intrinsic luminescence, causing decrease of the light output [8]. In addition to the luminescence measurement cited above [5], the Mo impurity was also found and characterized by means of ESR: x-ray irradiation of undoped $ZnWO_4$ at 20 or 77 K created paramagnetic Mo^{5+} ions [9] by electron transfer to Mo^{6+}. This Mo defect is stable at these temperatures and preserves the original C_2 symmetry of the W site. Also W^{5+} centres can be formed by x-ray or UV irradiation at 77 K; however, they are stable only near impurities (e.g. a substitutional OH^- ion [10]) reducing the centre symmetry to C_1. A number of defects like V_{Zn} (Zn vacancy), the Li^+ (probably also Na^+) impurity on the Zn site and the V_{Zn}–OH^- pair were shown to trap holes, forming very similar colour centres [9, 11, 12]. Under high-energy electron irradiation at 300 K, electrons are captured by oxygen vacancies creating $V_O^{\bullet}$ centres [11].

With the exception of the trapped hole on V_{Zn} and the $V_O^{\bullet}$ centre, all defects found up to now in $ZnWO_4$ are impurity-related defects. In this work we extended the study of colour centres by irradiating $ZnWO_4$ samples at 20 K with x-rays: a new hole-type intrinsic defect was found, characterized by ESR and ENDOR methods and attributed to the self-trapped hole in $ZnWO_4$. The study of its thermal stability, using models of the new and previously known defects, contributes to the understanding of the luminescence and thermoluminescence processes.

2. Experimental procedure

Single crystals of $ZnWO_4$ were grown in Budapest (Hungary) by a balance-controlled Czochralski technique using Pt crucibles [13]. The raw materials were analytical grade ZnO (REANAL) and WO_3 chemically produced from analytical grade Na_2WO_4 [14]. A 150 kV, 20 mA x-ray source was employed (irradiation times up to 1.5 h) in conjunction with ESR and ENDOR measurements carried out using a BRUKER Spectrometer (Model ESP 300 E) in Giessen (Germany). Three-dimensional (3D) TL measurements were made at the University of Sussex (Brighton, UK) where the x-ray irradiation was carried out using a 30 kV, 10 mA source at ∼15 K for 10 min. The heating rate was 6 K min^{-1}.

3. Results and discussion

3.1. Spin-Hamiltonian parameters

Prior to any irradiation, traces of Fe, Cr, Mn, Co, Cu, Rh and Pt impurity ions were detected in $ZnWO_4$ using ESR spectroscopy, in agreement with earlier results [7]. X-ray irradiation at 20 K induced a new paramagnetic defect whose ESR spectrum consisted of two line groups for arbitrary orientations of the magnetic field $\boldsymbol{B}$. This splitting, due to the existence of two energetically equivalent but magnetically non-equivalent centre sites (the $ZnWO_4$ crystal is monoclinic with space group $P2/c$ or C_{2h}^4), is typical for a centre in C_1 symmetry. For $\boldsymbol{B}$ inside the (010) plane or $\boldsymbol{B}$ along crystallographic directions, these two spectra coincide, as is to be

expected (more about the crystal structure and its consequences for the ESR spectra can be found in reference [7]). The average effective g-value was greater than the free-electron value g_e ($g_{av} \geqslant g_e = 2.0023$) and thus the new paramagnetic defect should be a hole, essentially an O^- centre. This assignment is also consistent with the observed C_1 centre symmetry and $S = 1/2$ as will be shown below.

The ESR spectrum of the O^- centre is shown in figure 1(a) for $\boldsymbol{B} \parallel [100]$. Symmetrically around the most intense central line, three different doublets with splittings marked A_1, A_2 and A_3 are seen with approximately the same moderate intensity. These doublets are obviously due to superhyperfine (SHF) interactions, most probably with three different W neighbours

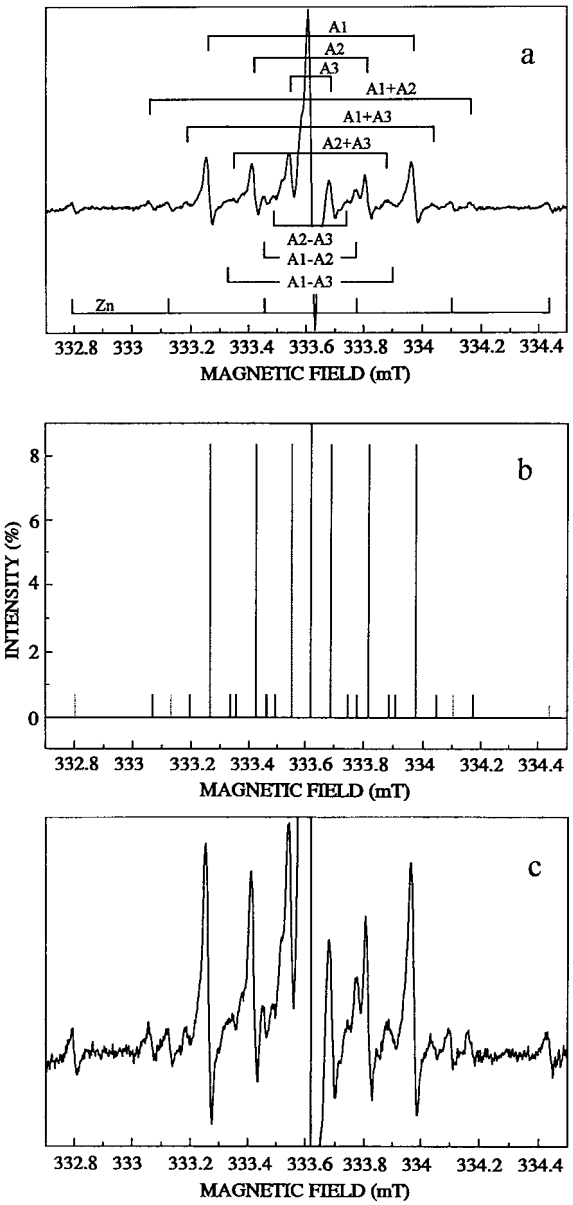

Figure 1. The ESR spectrum of the self-trapped hole centre in $ZnWO_4$ after x-ray irradiation at 20 K for 40 min. The observation was made at 4.4 K for $\boldsymbol{B} \parallel [100]$. Spectrum (a) is an experimental overview showing three different doublet splittings each arising from a single ^{183}W nucleus with non-zero nuclear spin (marked A_1, A_2 and A_3), splittings arising from simultaneous SHF interactions with two ^{183}W nuclear spins (marked $A_1 \pm A_2$, $A_1 \pm A_3$ and $A_2 \pm A_3$) and the ^{67}Zn sextet splitting. Spectrum (b) is a simulated ESR spectrum for three different interacting ^{183}W nuclei. Spectrum (c) is the same as (a) but magnified.

(hereafter they will be designated as W_1, W_2 and W_3, respectively). ^{183}W has a natural abundance of 14.28% and a nuclear spin of $I = 1/2$, explaining the doublets. Most of the holes are trapped near even W isotopes (85.72%, $I = 0$); therefore no SHF interaction is expected. Unfortunately a direct verification of the ^{183}W species causing the SHF interactions is not possible from the intensity ratios because of the different saturation behaviours of the central and satellite lines.

The ENDOR method is usually excellent for identifying the interacting nucleus. For small nuclear Zeeman interaction (smaller than the SHF splitting, as in the present case), the two ENDOR lines due to $m_s = \pm 1/2$ are centred to first order at $A/2$ and separated by twice the Larmor frequency of the interacting nucleus ($2\nu_n$). Figure 2 shows the ENDOR spectrum of the O^- centre for $\boldsymbol{B} \parallel [010]$. At this orientation the effective values found for A_1 and A_2 were approximately identical in the ESR spectrum. Due to the higher resolution of the ENDOR method the corresponding ENDOR lines are, however, resolved. For the W_1 nucleus the lines are centred at $A_1/2 = 7.676$ MHz and the separation is $2\nu_{n1} = 1.189$ MHz, while for W_2 the corresponding values are $A_2/2 = 7.145$ MHz and $2\nu_{n2} = 1.174$ MHz. The Larmor frequency of ^{183}W taken from the Bruker table is 0.62848 MHz at a magnetic field of 350 mT. The ENDOR measurement was done at 332.954 mT; at this magnetic field the expected ^{183}W Larmor frequency is 0.597 87 MHz and thus $2\nu_n = 1.195\,74$ MHz. The close agreement of the latter value with those of the experimental $2\nu_{n1}$ and $2\nu_{n2}$ unambiguously identifies the ^{183}W nucleus as responsible for the ESR satellites with splittings marked A_1 and A_2, respectively (figure 1(a)).

The third and weakest interaction with the W_3 nucleus could not be observed by means of ENDOR. In order to also attribute this interaction to a ^{183}W nucleus, we took further smaller

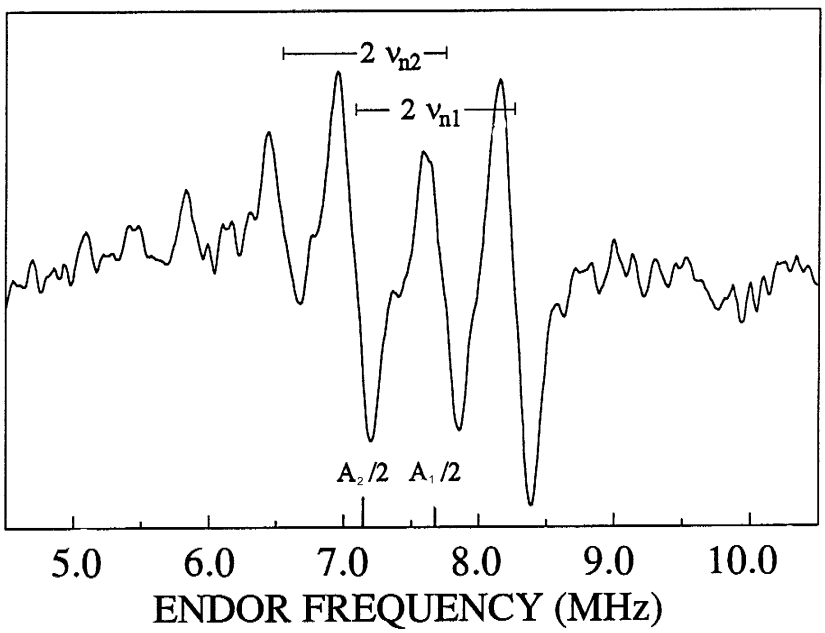

Figure 2. The ENDOR spectrum of the self-trapped hole centre in $ZnWO_4$ measured on the lowest-field single SHF line (at 332.954 mT) for $\boldsymbol{B} \parallel [010]$ at 4.4 K. The doublet separations are denoted by $2\nu_{n1}$ and $2\nu_{n2}$, while the centres of the doublets are denoted by $A_1/2$ and $A_2/2$, corresponding to the W_1 and W_2 SHF interactions, respectively.

ESR lines into consideration in addition to the central line and the three doublets in figure 1(a). These smaller lines are easy to recognize in the magnified spectrum in figure 1(c). Up to now we have considered those SHF lines corresponding to centres where only *one* ^{183}W nucleus was present near the hole centre. However, there exist also such centres in which the hole has *two* ^{183}W neighbours, which means that *two* non-zero nuclear spins interact simultaneously with the hole. Since the probability of the occurrence of these centres is much smaller, their ESR lines must have smaller intensity. These specific splittings are also indicated in figure 1(a) with $A_1 \pm A_2$, $A_1 \pm A_3$ and $A_2 \pm A_3$, respectively. The possible combinations, their probabilities, line numbers and intensity ratios relative to the central line (indicated by index c) are calculated using the equation

$$\frac{I}{I_c} = \frac{P}{nP_c} \tag{1}$$

and are given in table 1 assuming that the W_3 interaction is also due to a ^{183}W nucleus. The simulated stick diagram is shown in figure 1(b). From the agreement of observed and expected intensity ratios of lines due to two interacting nuclei and those due to a single interacting nucleus (see figures 1(b) and 1(c)) it is clear that the W_3 interaction also arises from a ^{183}W nucleus.

Table 1. Nuclear spins, line numbers, probabilities and intensity ratios for different ^{183}W SHF interactions.

Interacting nucleus	m_I (W_1)	m_I (W_2)	m_I (W_3)	Number of lines (n)	Probability (P)	Intensity ratio (I/I_0, %)
None	0	0	0	1	0.8572^3	100
W_1	$\pm$ 1/2	0	0	2	0.1428×0.8572^2	8.33
W_2	0	$\pm$ 1/2	0	2	0.1428×0.8572^2	8.33
W_3	0	0	$\pm$ 1/2	2	0.1428×0.8572^2	8.33
$W_1 + W_2$	$\pm$ 1/2	$\pm$ 1/2	0	4	$0.1428^2 \times 0.8572$	0.69
$W_1 + W_3$	$\pm$ 1/2	0	$\pm$ 1/2	4	$0.1428^2 \times 0.8572$	0.69
$W_2 + W_3$	0	$\pm$ 1/2	$\pm$ 1/2	4	$0.1428^2 \times 0.8572$	0.69

In addition to the lines with two interacting W nuclei, one can distinguish six further lines with similar intensity (figures 1(a)–1(c)). These lines are presumably due to zinc: the ^{67}Zn isotope has $I = 5/2$ with a natural abundance of 4.1%. The expected intensity ratio of such lines relative to the central line is 0.71%. These SHF lines were not studied in further detail because of their low intensities.

In order to determine the spin-Hamiltonian parameters of the present O^- centre, angular dependencies of the central ESR lines and the W_1 and W_2 ENDOR spectra have been measured in four different planes. They are shown for three crystallographic planes in figures 3(a)–3(c) and figures 4(a)–4(c), respectively. In figure 3(c), where the rotation was made in the (100) plane, the slight separation of the two spectra was only due to a small sample misorientation. The following spin Hamiltonian was employed:

$$\mathcal{H}_s = \mu_B \boldsymbol{S} \cdot \tilde{\mathbf{g}} \cdot \boldsymbol{B} + \sum_{i=1}^{n} (\boldsymbol{S} \cdot \tilde{\mathbf{A}}_i \cdot \boldsymbol{I}_i - g_N \mu_N \boldsymbol{B} \cdot \boldsymbol{I}_i) \tag{2}$$

with $S = 1/2$ and $I = 1/2$, where n is the number of interacting nuclei. The central ESR lines correspond to the W and Zn isotopes with $I = 0$; thus for the determination of the $\tilde{\mathbf{g}}$-tensor components only the electron Zeeman term should be calculated, without the SHF and

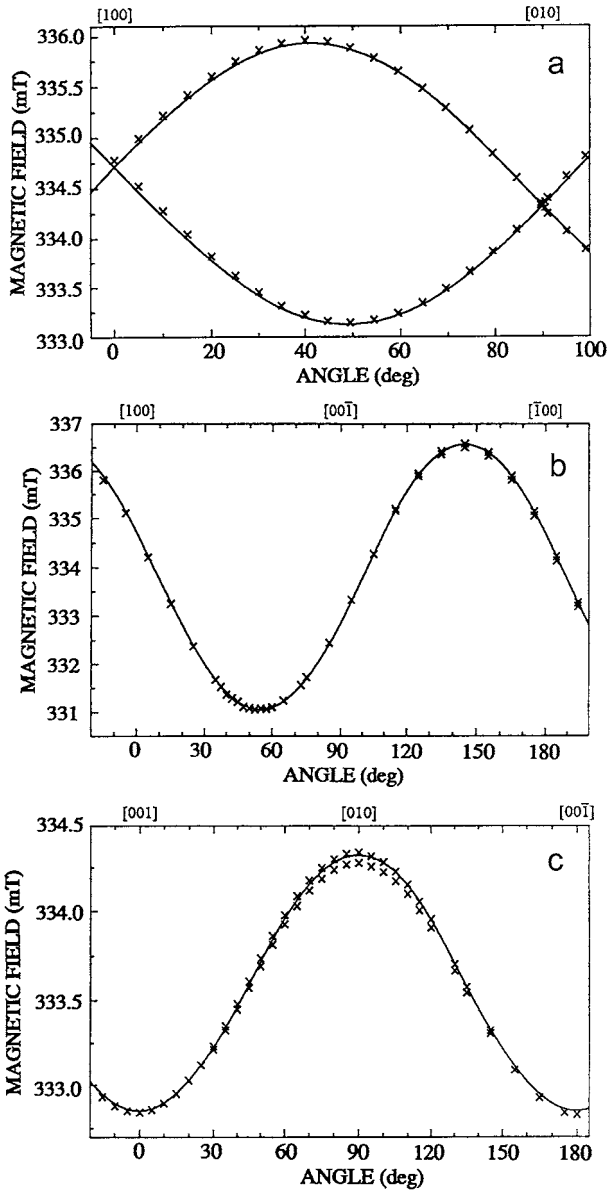

Figure 3. ESR angular variations for the two sites of the intrinsic O^- centre in $ZnWO_4$. The angular dependencies (a), (b) and (c) correspond to the rotation of B in the (001), (010) and (100) planes, respectively (note the difference in horizontal scales). Crosses represent experimental data for the central lines and the solid curves are computer-simulated angular variations for the same lines calculated with the optimized $\tilde{\mathbf{g}}$-tensor spin-Hamiltonian parameters.

nuclear Zeeman terms. For fitting the ENDOR experimental data in equation (2), the electron Zeeman, SHF and nuclear Zeeman terms for only one nucleus (the W_1 or W_2 nucleus) should be considered (these interactions can be treated separately since in each contributing centre there is only one ^{183}W interacting with the hole). The computer fit parameters are listed in table 2.

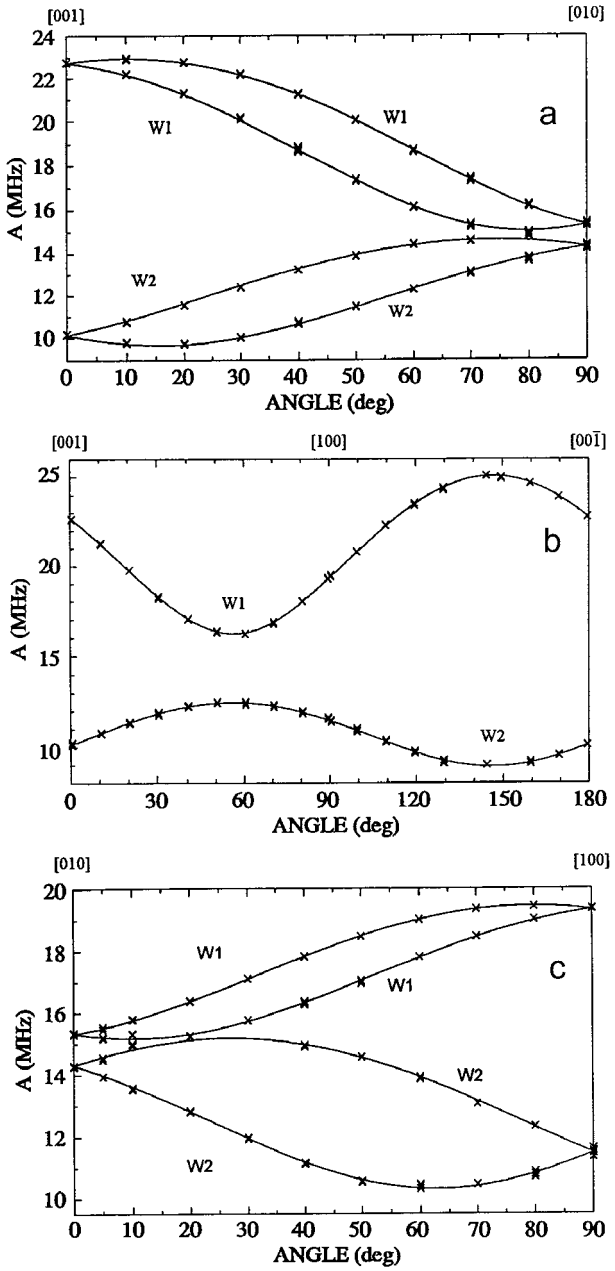

Figure 4. Angular variations of the ^{183}W SHF splittings A_1 and A_2 derived from ENDOR for the W_1 and W_2 neighbours of the self-trapped hole centre in $ZnWO_4$ at 4.4 K. The angular variations of the two geometrical sites (a), (b) and (c) are shown for each SHF interaction for the rotation of $\boldsymbol{B}$ in the (100), (010) and (001) planes, respectively (note the difference in horizontal scales). Crosses represent experimental data and the solid curves are computer-simulated angular variations calculated with the optimized spin-Hamiltonian parameters.

In $ZnWO_4$, the W and Zn ions are each surrounded by six oxygen ions, pairwise, equidistantly: the long, medium and short W–O distances are 0.2133, 0.1914 and 0.1789 nm

Table 2. Best-fit spin-Hamiltonian parameters of the self-trapped hole centre in $ZnWO_4$ single crystals. The A(SHF) principal values are given in units of MHz. $\tilde{\mathbf{A}}$ was also transformed into another useful form, where a is the isotropic hyperfine coupling constant (proportional to the spin density on the specific nucleus), b is the dipole–dipole interaction in axial symmetry and b' is the measure of its deviation from axial symmetry. The direction cosines of the dimensionless eigenvectors are defined with respect to the crystallographic axes [100], [010] and [001], respectively, and their estimated errors are ±0.005.

g_{xx}	g_{yy}	g_{zz}			
$\tilde{\mathbf{g}}$	2.0406 ± 0.0002	2.0213 ± 0.0002	2.0030 ± 0.0002		
Eigenvectors	−0.597	−0.192	0.779		
	0.234	0.887	0.398		
	0.767	−0.420	0.484		
	A_{xx}	A_{yy}	A_{zz}	a	b	b'
$\tilde{\mathbf{A}}_1$	14.00 ± 0.15	17.33 ± 0.15	25.09 ± 0.15	18.81	3.14	1.66
Eigenvectors	0.468	−0.699	−0.541			
	−0.802	−0.593	0.073			
	0.372	−0.400	0.838			
$\tilde{\mathbf{A}}_2$	8.91 ± 0.15	10.76 ± 0.15	15.65 ± 0.15	11.77	1.94	0.93
Eigenvectors	−0.568	−0.679	−0.466			
	−0.017	−0.557	0.831			
	0.823	−0.480	−0.305			

and the Zn–O distances are 0.2227, 0.2090 and 0.2026 nm, respectively [16]. There are two energetically different oxygen ions: the first one (marked A in figure 5) is bound to two Zn ions (long and medium Zn–O bonds) and one W ion (short W–O bond) while the second one (marked B in figure 5) is connected with two W ions (medium and long W–O bonds) and one Zn ion (short Zn–O bond). Since we observed SHF interactions with a single Zn nucleus and two stronger interactions with W nuclei, it is obvious that we can assume that the hole is centred at an oxygen position of B type: in figure 5 the O^- centre is shown in one of the possible magnetically non-equivalent sites denoted by I. The third resolved SHF interaction (W_3) arises from a more distant W nucleus. The a_1/a_2 ratio (a_1 and a_2 are the isotropic SHF constants given as $a_i = \frac{1}{3}\,\mathrm{Tr}\,\tilde{\mathbf{A}}_i$) of the two larger tungsten SHF interactions derived from the data in table 2 is 1.6 and this ratio is 1.5 times smaller than that for a similar hole centre in $CaWO_4$ [17], where the absolute a-values are also bigger. This is an indication of the stronger bonding within the isolated WO_4 tetrahedra of the scheelite structure and on the other hand makes clear how much the isotropic SHF splitting in tungstate materials depends on the actual distribution of the hole wavefunction. The above centre model is further supported by the coincidence (within 10°) of the main axes of the $\tilde{\mathbf{A}}_1$- and $\tilde{\mathbf{A}}_2$-tensors with the directions of the medium and long W–O bonds, respectively. Since no impurity SHF interaction was observed, the centre may be regarded as the self-trapped hole centre.

It is interesting to note that for all models of hole-type defects in $ZnWO_4$ studied up to now (O^-–V_{Zn}, O^-–V_{Zn}–OH^- and O^-–Li_{Zn}) [9,11,12], the O^- centre is at the same oxygen position B. This shows the consistency of the models and clearly indicates site B as the energetically most favourable location for a hole.

In addition to the intrinsic hole centre, electron-type defects were also produced by x-ray irradiation at 20 K: the paramagnetic Mo^{5+} centre with C_2 symmetry [9] was observed,

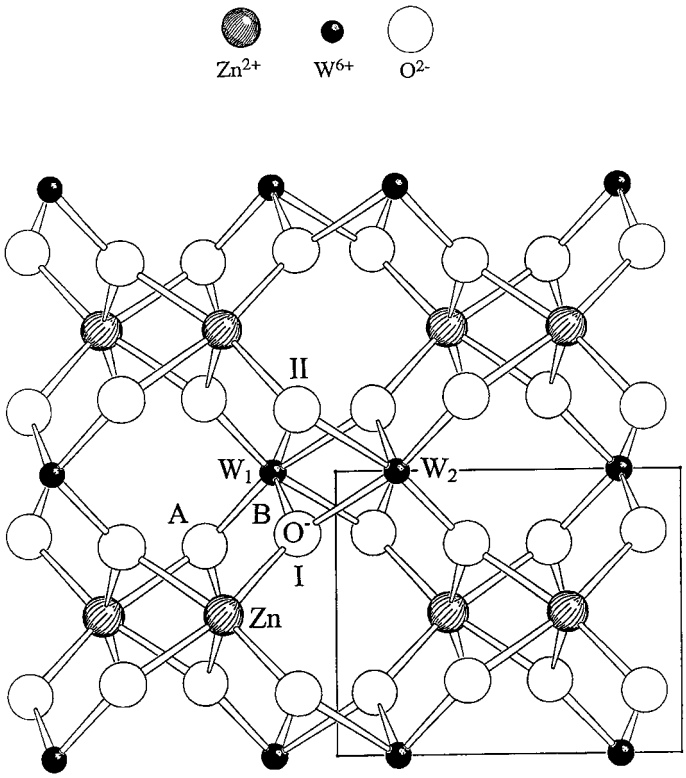

Figure 5. The projection of the model of the self-trapped hole centre in $ZnWO_4$ onto the (001) plane. The two energetically different O positions in $ZnWO_4$ are marked A and B; the two energetically equivalent but magnetically different O sites (resulting for arbitrary orientation in two different ESR and ENDOR spectra of the same centre with C_1 symmetry) are marked I and II. The framed part represents the unit cell. The crystal model was drawn employing the SCHAKAL 92/V256 program (Kristallographisches Institut Freiburg).

and the intensity of the Fe^{3+} ESR spectrum decreased, indicating the formation of Fe^{2+} ions. It should be assumed that one or more diamagnetic electron-type centres were also created. These defects may serve as charge-compensating defects for the O^- centres.

3.2. Temperature effects in the ESR spectra

The ESR spectrum of the present centre has an interesting temperature dependence. On raising the temperature above 33 K, the C_1 symmetry observed at lower temperatures averages to C_2 symmetry (figure 6). First the broadening of the two central lines can be observed in figure 6 up to 27 K. The lines start to shift towards each other (averaging of g) from 29 K; the final result is a single line between the two original central lines. Above 35 K, motional narrowing is observable. These changes are fully reversible. However, the spectrum of the centre starts to decrease irreversibly at ∼50 K and completely disappears at about 75 K with the simultaneous formation of different impurity-related hole-type defects like the O^-–V_{Zn}–OH^- centre [9], O^-–Mo^{6+} (which has not yet been studied in detail) and O^-–Li^+ or its variant with the Na^+ ion [12]. These centres are assigned to O^- hole centres captured at a zinc vacancy–OH^- pair, at a Mo^{6+} ion and at a Li^+ (or Na^+) ion, respectively.

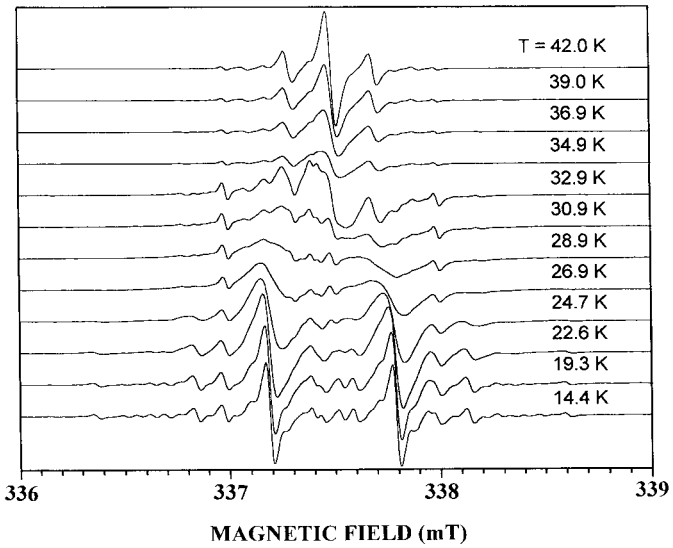

Figure 6. ESR spectra of the self-trapped hole centre in $ZnWO_4$ at different temperatures in the (001) plane, $\sim 5^\circ$ away from $\boldsymbol{B} \parallel [100]$ where the two different spectra are resolved at low temperature.

The symmetry change can be explained by a motional averaging effect. The hole starts to jump between two possible, energetically equivalent O sites (marked I and II in figure 5) reorienting the centre, causing the shift of the central lines (averaging of g) and line broadening. The hopping frequency can be expressed by the following equation:

$$\nu_h = \nu_0 \mathrm{e}^{-E/(kT)} \tag{3}$$

since the reorientation is thermally activated. E is the activation energy for a jump and ν_0 is the attempt frequency. Investigating the linewidth broadening, ν_h can be expressed by the following equation:

$$\nu_h = (\Gamma - \Gamma_0) 2\gamma_e \tag{4}$$

where Γ_0 is the linewidth at low temperature without thermally activated hopping and Γ is the actual linewidth; γ_e is the electronic gyromagnetic ratio [18]. For the line shift the following expression can be considered:

$$\nu_h = \sqrt{(\delta B_0)^2 - (\delta B)^2}\,\frac{\gamma_e}{\sqrt{2}} \tag{5}$$

where δB_0 is the line separation at low temperatures without hopping and δB is the actual line separation [18] measured in mT. Figure 7 shows the logarithmic plots of ν_h derived on the basis of equations (4) and (5), respectively, as functions of T^{-1}. From the slopes, E can be determined. The experimental points are reasonably close to parallel straight lines, yielding 0.016 ± 0.003 eV and $\nu_0 \sim 4 \times 10^{10}$ Hz. The hopping frequency at 25 K where the effect is most conspicuous in ESR is $\nu_{h25} = 2 \times 10^7$ Hz.

Above 50 K the holes may acquire energies exceeding the bonding (self-trapping) energy and become free. The self-trapped holes completely disappear at $\sim$75 K. A fraction of them recombine with electron-type defects contributing to the TL while another fraction are recaptured at various impurities (V_{Zn}–OH^- pairs, Li^+ or Na^+ and Mo^{6+} ions). The latter hole-type centres have different thermal stabilities; however, none of them are stable above 130 K.

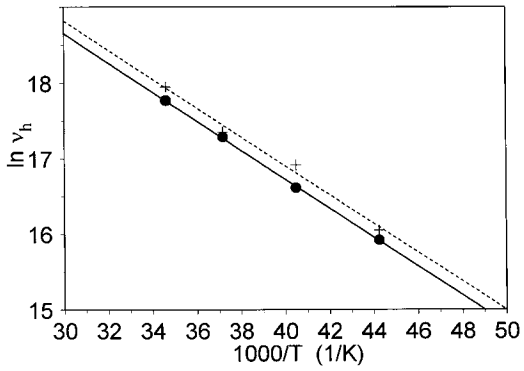

Figure 7. A semilogarithmic plot of the hopping frequency ν_h, calculated from the ESR linewidth change using equation (4) (crosses) and from the line position shift using equation (5) (squares), of the intrinsic O^- centre in $ZnWO_4$ versus reciprocal temperature, with nearly coinciding linear fits (solid lines).

The low stability of the present O^- centre and the lack of any resolved impurity-related SHF interaction in its ESR spectrum suggest that the defect is intrinsic; i.e. at least in its nearest neighbourhood, there is no impurity ion. This hypothesis is strongly supported by the observed oscillating mechanism of the hole which would be impossible if an impurity were nearby: positions I and II would not be energetically equivalent if an impurity were either near to I or near to II (it is very unlikely that both positions are associated with impurities at specific distant sites making both positions equivalent).

3.3. Contribution to the model of the TL mechanism

As far as we are aware, up to now thermoluminescence curves for $ZnWO_4$ have been measured only for samples irradiated at 77 K. We repeated the TL measurements after x-ray irradiating our sample at 15 K, obtaining the spectra shown in figure 8. The TL peaks above 150 K are obviously due to Mo impurity-related centres since they are enhanced for Mo-doped crystals.

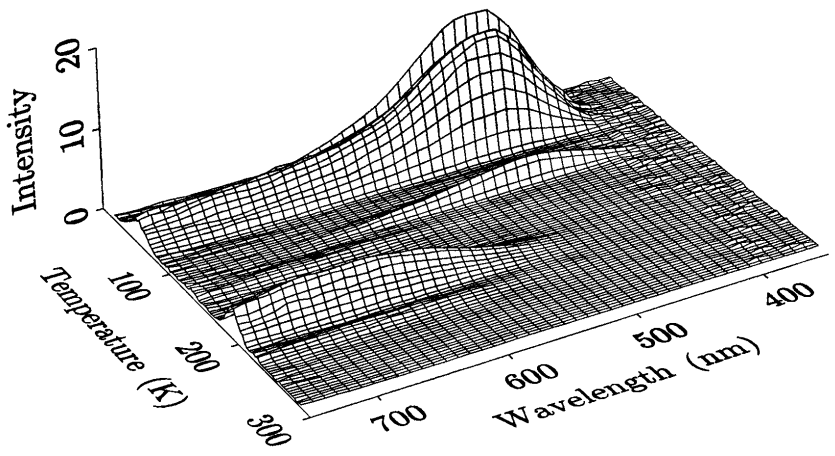

Figure 8. The 3D-TL spectrum of an undoped $ZnWO_4$ sample x-ray irradiated at 15 K for ten minutes.

Further on, the three-dimensional TL spectrum shows typical emission curves of Mo identified in photo-illuminated $ZnWO_4$:Mo in the range 600–700 nm [5] and so the Mo centres cannot be the luminescence centres giving the blue-green emission. However, the rest of the TL peaks are accompanied by emission at ∼480 nm, well known in $ZnWO_4$. Since two groups of glow peaks in different temperature ranges have their emission maxima at this wavelength, the self-trapped hole described here (unstable above ∼50 K) and one of the impurity-related O^- centres (created above 50 K) can be ruled out as possibilities for the basic luminescence centre. It is much more likely that an electron-type defect emits ∼480 nm light at different temperatures when one of the hole centres becomes unstable, with the hole moving in the valence band until it reaches the electron-type defect and recombines with an electron. This process will give the same emission at different temperatures whenever a hole-type defect becomes unstable and recombines with the same kind of electron-type luminescence centre.

As mentioned above, Fe^{2+} is an electron centre in the crystal studied. Since, however, earlier luminescence studies showed the intrinsic nature of the luminescence, this centre can be ruled out with high probability as the possible source of the ∼480 nm emission. The same holds for the $V_O^{\bullet}$ centre since it cannot be created by x-ray irradiation. The fact that no other intrinsic paramagnetic electron-type centres were ever observed in x-ray-irradiated $ZnWO_4$ indicates the possibility that some diamagnetic centre could be the common recombination partner.

4. Summary

In $ZnWO_4$ x-ray irradiated at 20 K, an intrinsic hole centre was identified by ESR and ENDOR spectroscopy with principal g-values typical for O^- centres. Relatively strong SHF interactions with two W and one Zn ion give information about the neighbourhood of the O^- ion: it resides at the B-type oxygen position which has one nearest Zn and two nearest W ions. The defect becomes thermally unstable near 50 K and disappears completely above 75 K. The present O^- centre is believed to be the intrinsic self-trapped hole in $ZnWO_4$ because of its low stability, the lack of any impurity-related SHF interaction in its ESR spectrum and the hopping mechanism observed above ∼20 K.

Broadening of the lines and averaging of the g-value is observed which is explained as caused by thermally activated hopping of the hole between two energetically equivalent oxygen positions. The activation energy of this reorientation is found to be 0.016 ± 0.003 eV.

Since the intrinsic O^- centre partly recombines and partly converts into other types of hole centre, it cannot be the luminescence centre giving the typical emission at ∼480 nm in $ZnWO_4$, which occurs at different temperatures both below and above 75 K. Therefore an electron-type defect should be the luminescence centre yielding the same emission, recombining with holes at temperatures where any of the hole-type centres becomes unstable. Since earlier luminescence studies demonstrated its intrinsic nature, the luminescence centre may be assumed to be some intrinsic diamagnetic electron-type defect.

Acknowledgments

We are grateful to Professor P D Townsend for his assistance at the University of Sussex, where the TL measurements were conducted, and Ms Á Péter, Ms Zs Tóth and Mr Gy Matók for growing and processing the samples. This research was supported by the Deutscher Akademischer Austauschdienst (DAAD Germany) and the National Science Research Fund (OTKA Hungary) (Grant No T22859).

References

[1] Ishii M and Kobayashi M 1991 *Prog. Cryst. Growth* **23** 245
[2] Grabmaier B C 1984 *IEEE Trans. Nucl. Sci.* **31** 372
[3] Wang H, Medina F D, Liu D D and Zhous Y D 1994 *J. Phys.: Condens. Matter* **6** 5373
[4] *Gmelin Handbuch der Anorganischen Chemie, W Ergänzungsband B Oxide* 1980 ed H Katscher (Berlin: Springer) pp 177–92
[5] Földvári I, Kappers L A, Gilliam O R, Hamilton D S, Lyu Li-Ji, Cravero I and Schmidt F 1990 *J. Chem. Phys. Solids* **51** 953
[6] Ovechkin A E, Ryzhikov V D, Tamulaitis G and Zukauskas A 1987 *Phys. Status Solidi* a **103** 285
[7] Watterich A, Edwards G J, Gilliam O R, Kappers L A, Madacsi D P, Raksányi K and Voszka R 1991 *J. Phys. Chem. Solids* **52** 449
[8] Watterich A, Gilliam O R and Kappers L A 1993 *Solid State Commun.* **88** 619
[9] Hofstaetter A, Raksányi K, Scharmann A, Schön F and Watterich A 1993 *Proc. 12th Int. Conf. on Defects in Insulating Materials (Nordkirchen, Germany, 1992)* vol 2, ed O Kanert and J-M Spaeth (Singapore: World Scientific) p 700
[10] Watterich A, Gilliam O R, Kappers L A and Raksányi K 1996 *Solid State Commun.* **97** 477
[11] Watterich A, Edwards G J, Gilliam O R, Kappers L A, Corradi G, Péter Á and Vajna B 1994 *J. Phys. Chem. Solids* **55** 881
[12] Watterich A and Hofstaetter A 1998 *Solid State Commun.* **105** 357
[13] Schmidt F and Voszka R 1981 *Cryst. Res. Technol.* **16** K127
[14] Földvári I, Péter Á, Keszthelyi-Lándori S, Capelletti R, Cravero I and Schmidt F 1986 *J. Cryst. Growth* **79** 714
[15] Spaeth J-M, Niklas J R and Bartram R H 1992 *Structural Analysis of Point Defects in Solids* (New York: Springer)
[16] Schofield P F, Knight K S and Cressey G 1996 *J. Mater. Sci.* **31** 2873
[17] Biederbick R, Born G, Hofstaetter A and Scharmann A 1975 *Phys. Status Solidi* b **69** 55
[18] Weil J A, Bolton J R and Wertz J E 1994 *Electron Paramagnetic Resonance* (New York: Wiley)